Multicomponent Reactions

DOI: 10.1002/ange.201001343

Robust Generation of Lead Compounds for Protein–Protein Interactions by Computational and MCR Chemistry: p53/Hdm2 Antagonists**

*Anna Czarna, Barbara Beck, Stuti Srivastava, Grzegorz M. Popowicz, Siglinde Wolf, Yijun Huang, Michal Bista, Tad A. Holak, and Alexander Dömling**

In memory of Ivar Ugi

The discovery of a lead compound is an essential process in early drug discovery, hopefully eventually resulting in a clinical candidate and a drug for the treatment of a disease. Besides affinity and selectivity for the target, however, other target-unrelated compound properties are equally important for the fate of a drug candidate, for example, water solubility, lipophilicity, and molecular weight since they determine important aspects such as oral bioavailability, dosing schedule, and side effects. The parallel discovery and early development of several leads is therefore now pursued whenever possible, an approach that takes into account the high attrition rate of early drug discovery projects. Currently, hits as starting points for medicinal chemistry optimizations are mostly found by high-throughput screening (HTS) campaigns and to a much lesser extent by structure-based approaches including fragment-based and computational drug discovery. For certain target classes, however, HTS often yields very low numbers of hits.[1] For example, protein–protein interactions (PPIs) are notoriously difficult to hit with druglike small molecules.[2] This has been assigned to the unusual structure, topology, and flexibility of protein–protein interfaces.[3] The fact that several drugs targeting PPIs have recently entered the clinical development clearly shows that certain PPIs, for example, between Bcl-x and XIAP, can be efficiently targeted by small molecules.[4] Herein, we describe a complementary process that led to the parallel discovery of several compounds belonging to seven different scaffold classes, amenable to synthesis by efficient multicomponent reaction (MCR) chemistry in just one step, which antagonize the PPI between the transcription factor p53 and its negative regulator Hdm2.

Protein–protein interactions are often mediated by only a few key amino acid side chains and the terms "hot spot" and "anchor" have been introduced for such locally constrained areas and amino acids on the surface of interacting proteins.[2,5,8] In a first approximation, the depth into which a specific amino acid side chain of the donor protein is buried in the acceptor protein is indicative of its energetic importance. We reasoned that this "anchor" amino acid side chain might serve as a reasonable starting point for the design of (ant)agonists of a PPI. Thus, we use this particular amino acid side chain as an initial anchor in virtual libraries of low-molecular-weight scaffolds. Virtual compounds containing anchor side chains are selected for synthesis and screening based on their docking into the PPI interface. The starting point for the docking/energy minimization procedure is chosen in such a way that an overlap between the anchor and the template amino acid side chain is ensured. In order to rapidly test these ideas, we chose an efficient and fast but versatile synthetic approach, MCR (Figure 1).[6] MCR allows for the assembly of many diverse and complex scaffolds in a one-step/one-pot manner, thus saving time and resources, and potentially increasing the success rate of lead discovery.

The PPI interface of p53/Hdm2 has been characterized in molecular detail by X-ray structure analysis.[7] It relies on the steric complementarity between the Hdm2 cleft and the hydrophobic face of the p53 α-helix and, in particular, on a triad of p53 amino acids Phe19, Trp23, and Leu26, which insert deep into the Hdm2 cleft (Figure 1A in the Supporting Information). We chose the indole side chain of Trp23 as the anchor residue for three reasons: 1) it is the central amino acid of the triad, thus facilitating addressing by the antagonists the crucial Phe19 and Leu26 binding sites; 2) it is deeply buried in Hdm2; and 3) it also features, in addition to extensive van der Waals contacts, a hydrogen bond to the Leu54 backbone carbonyl oxygen of Hdm2. In fact, calculation of the solvent-accessible surface areas of all amino acids in the p53/Hdm2 interaction ranks Trp23 the highest (Trp23 > Phe19 > Leu26).[8] Next, from our in-house database of several hundred MCR scaffolds, we selected forty MCR scaffolds to create virtual compound libraries.[6] By design, each of the compounds incorporated the anchor. We used indole and bioistosteric 4-chlorophenyl derivatives[24] supplied with the corresponding functional groups as anchors to

[*] Dr. B. Beck, Dr. S. Srivastava, Y. Huang, Prof. A. Dömling
Departments of Pharmaceutical Sciences and Chemistry
University of Pittsburgh, Biomedical Science Tower 3
3501 Fifth Avenue, Pittsburgh, PA 15261 (USA)
Fax: (+1) 412-383-5298
E-mail: asd30@pitt.edu
Homepage: http://www.pitt.edu/~asd30/Doemling_lab.html
Dr. A. Czarna, G. M. Popowicz, S. Wolf, M. Bista, Prof. T. A. Holak
Max-Planck-Institut für Biochemie, Martinsried (Germany)

[**] MCR: multicomponent reaction. We thank Dr. Ulli Rothweiler for fruitful discussion. This work was supported by the NIH (grant 1R21M087617-01 to A.D.) and the Deutsche Krebshilfe (grant 108354 to T.H.) and is part of an NCI-RAND program. We thank Haixia Liu for the synthesis of PB3.

Supporting information for this article is available on the WWW under http://dx.doi.org/10.1002/anie.201001343.

WILEY InterScience DISCOVER SOMETHING GREAT
© 2010 Wiley-VCH Verlag GmbH & Co. KGaA, Weinheim

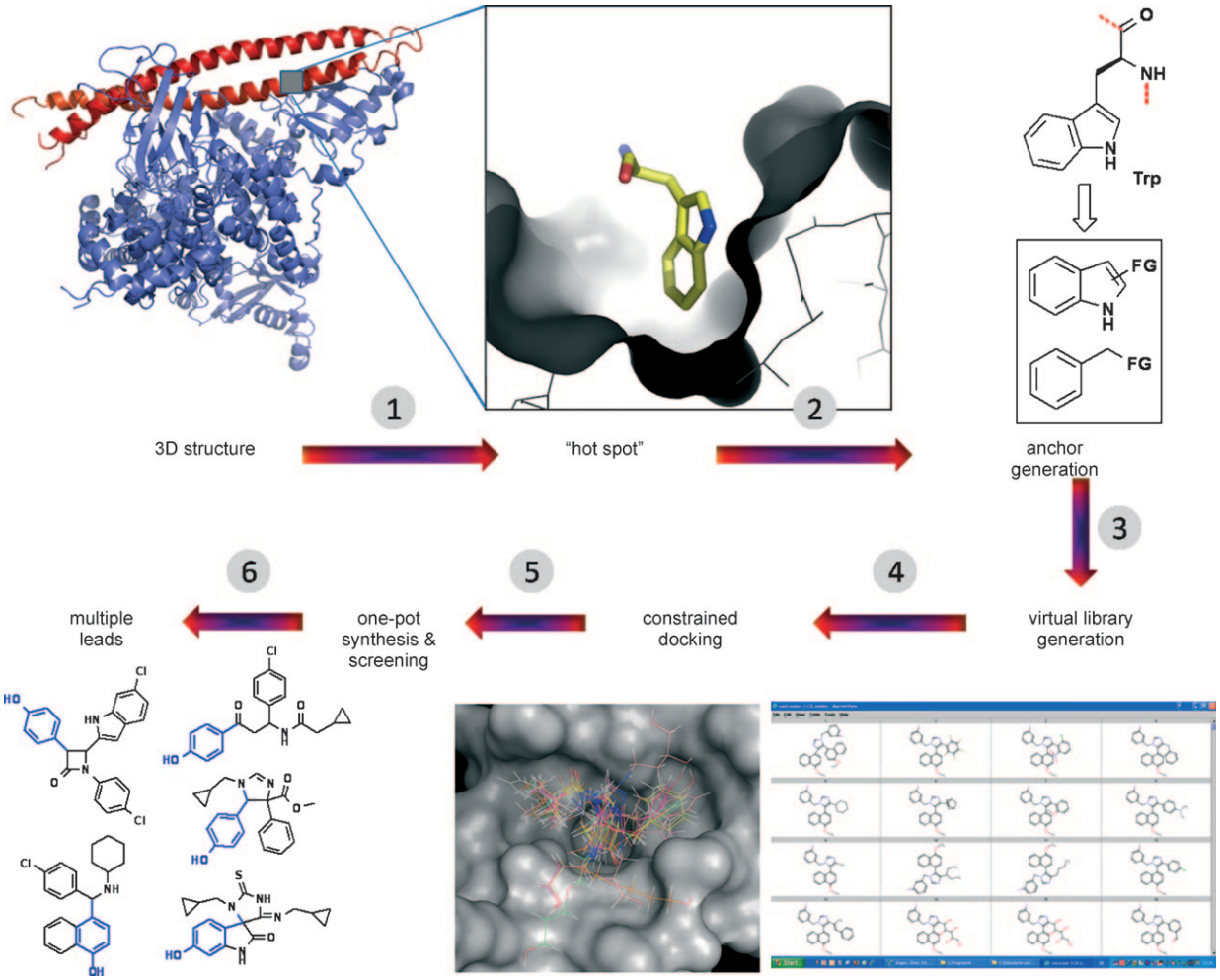

Figure 1. Graphical representation of the workflow for the rapid generation of low-molecular-weight (ant)agonists of PPIs. The process relies on high-resolution structural data of the target (1), the presence and identification of a highly buried amino acid (2), a fragmentation/anchor generation step (3), virtual chemistry employing the anchor and based on multicomponent reactions (4), constrained docking forcing the anchor fragment into the binding site (5), and synthesis and screening (6). (FG = functional group.)

act as starting materials for the MCRs (Supporting Information, Figure 1B); for example, we used unsubstituted indole and oxindole to perform a Friedel–Crafts-type alkylation and an Ugi four-component condensation, respectively (Supporting Information, Table 1).

The virtual library of compounds comprising all possible stereoisomers was generated using REACTOR software.[9] Different aliphatic and aromatic starting materials to represent different shapes and electrostatic features were chosen. The virtual libraries incorporating the anchor side chain were docked into a rigid model of the p53 binding site in the Hdm2 receptor (PDB identifier: 1YCR) using the modeling/docking software package Moloc.[7,10] Assuming that the anchor residue predefines the binding site of the molecules and in order to avoid nonproductive docking geometries, we forced the anchor part (indole or 4-chlorophenyl) of the compounds to overlap with the respective Trp23 anchor as a starting point for energy minimization. As an encouraging evidence for the anchor approach we solved the crystal structure of the MCR compound PB12 bound to Hdm2 (Figure 2).[11] This structure shows an almost perfect alignment of the Trp23 indole anchor

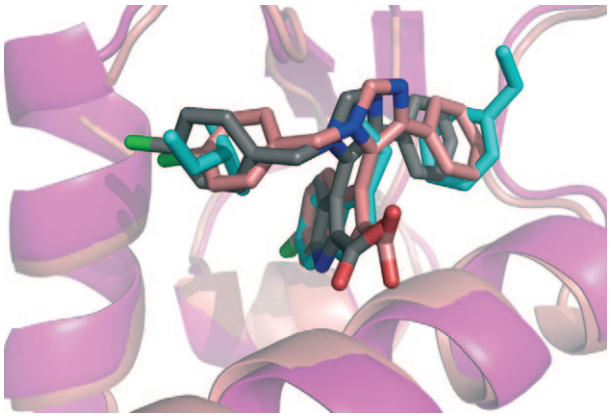

Figure 2. Alignment of the anchor p53 residues Phe19, Trp23, and Leu26 (cyan sticks) bound to Hdm2 (dark pink cartoon, PDB ID: 1YCR) with a van Leusen imidazole PB12 based antagonist (pink sticks) bound to Hdm2 (light pink cartoon, PDB ID: 3LBK) and the corresponding predicted docking geometry of PB12 (grey sticks).

© 2010 Wiley-VCH Verlag GmbH & Co. KGaA, Weinheim

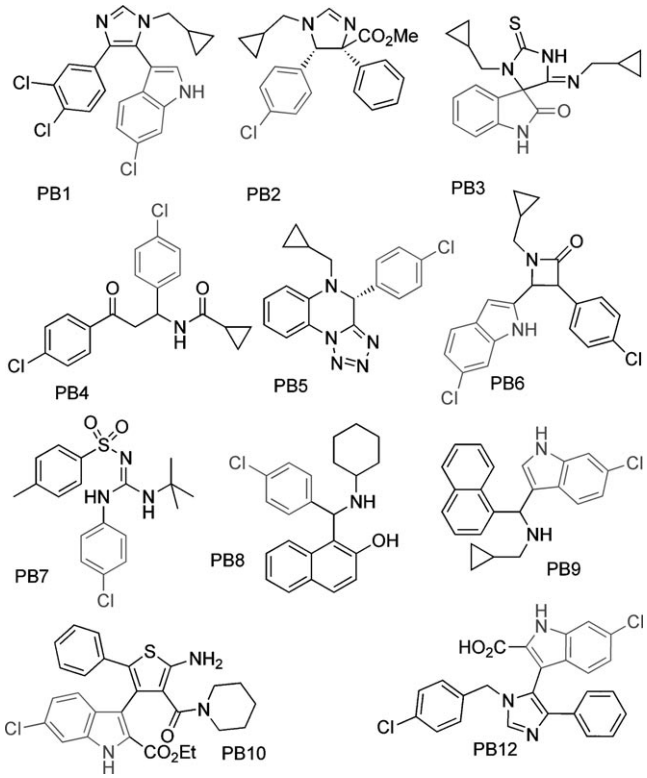

Scheme 1. Predicted and found p53/Hdm2 antagonists based on multiple MCR scaffolds (the anchor moiety is marked gray, PB = Pittsburgh).

with the indole moiety of PB12 (see Scheme 1) with an RMSD (indole) of 0.34 Å.

From the highest-ranking docked compounds, which addressed all three binding sites of p53 (Phe19, Trp23, and Leu26), we chose several compounds for synthesis and screening based on several features (Scheme 1). First, the compounds were chosen so as to belong to different types of scaffolds to ensure variation in backbones and chemistry. Second, we chose reactions for which the starting materials were commercially available or readily accessible by synthesis. As a third criterion, we preferentially chose MCRs we had used before.[6a] Products were synthesized according to two different Ugi MCR variations (PB3, PB5),[12] the van Leusen three-component reaction (PB1, PB12),[13] the Orru three-component reaction (PB2) followed by an amidation step (PB11),[14] the Passerini three-component reaction (PB9),[15] the Betti three-component reaction (PB8),[16] the Staudinger three-component reaction (PB6),[17] an MCR that formed an amidinosulfone amide (PB7),[18] the Gewald three-component reaction to an aminothiophene (PB10),[19] and an α-amidoalkylation (PB4).[20] Among the eleven different MCR series prepared, seven scaffolds showed binding activities less than 60 μM (Table 1).

Representative docking geometries of the predicted p53/Hdm2 antagonist compounds are shown in Figure 3 and in Figure 2 of the Supporting Information. Next, these compounds were screened for their ability to bind to Hdm2 and to antagonize the p53/Hdm2 PPI. We chose NMR spectroscopy for this test as it provides a wealth of information that

Table 1: NMR spectroscopically determined activities of predicted, synthesized, and tested compounds and known optimized compounds (fluorescent polarization (FP) assay).[a]

Compound	K_d [μM]	Compound	K_d [μM]
PB1	40 ± 15[b]	PB7	>100[b]
syn-PB2	3 ± 1[c]	PB8	60 ± 20[b,c]
anti-PB2	40 ± 10[b]	PB9	60 ± 30[b]
PB2a	2 ± 1[c]	PB10	5 ± 2[c] (11 ± 0.5)
PB3	20 ± 7[b,c]	PB11	0.8 ± 0.4[c]
PB4	30 ± 10[b]	PB12	1.1[c] (0.7 ± 0.04)
PB5	30 ± 10[c]	nutlin-3[d]	0.09 ± 0.03[c] (0.04 ± 0.01)
PB6	precipitation	MI-63[d]	0.01 ± 0.01[c] (0.003 ± 0.002)

[a] Errors for the FP values are determined by fit confidence. The experimental error of K_d measured by NMR was assumed to be ca. 30%. The techniques used for [b] and [c] gave the same values within the error boundaries. [b] Binary titration of the ligand with apo-^{15}N-Hdm2 using ^{15}N-HSQC.[22] [c] AIDA experiment.[23] [d] Nutlin-3 and MI-63 are described in Ref. [24] and Ref. [11, 25], respectively; the K_d values are our measurements, in agreement with Ref. [11, 24, 25, 26].

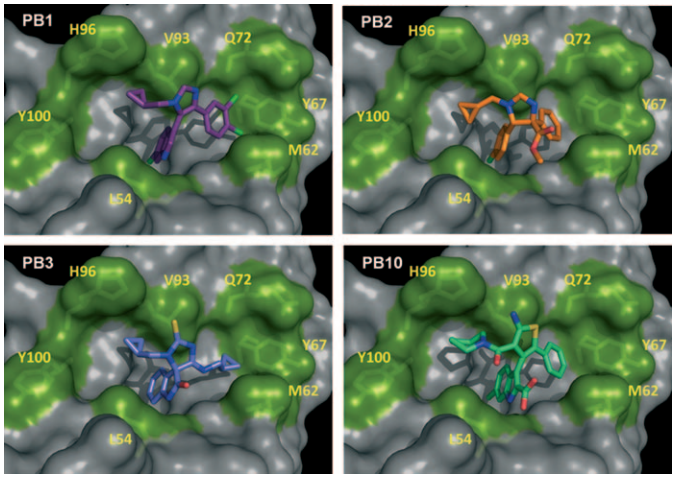

Figure 3. Binding models of four p53/Hdm2 antagonists by constrained docking into PDB 1YCR: 5-indoloimidazole PB1; imidazoline PB2; thiohydantoinimide PB3; and 2-aminothienyl-3-acetamide PB10. Several rim key amino acids of Hdm2 are shown as sticks and green surface and numbered. The docking models are in accordance with the observed Hdm2 HSQC NMR shifts obtained from titrations. All geometries show the receptor in the same orientation as in Figure 2.

otherwise cannot be assessed in high-throughput assays. Importantly, use of NMR-based screening allowed for determination of both compound affinity to Hdm2 and the ability of a compound to dissociate the preformed p53/Hdm2 complex. Other important questions about the compound properties can also be answered with an NMR-based approach. These include: Is the compound sufficiently water soluble? Does the compound bind to Hdm2 or to p53? Does the compound cause precipitation of any of the proteins? Does the compound lead to major conformational changes in the binding protein? What is the binding site of the compound on the protein surface?

All of this information is instrumental in order to optimize a compound series not only for potency and selectivity but also for, for example, water solubility and protein binding.

© 2010 Wiley-VCH Verlag GmbH & Co. KGaA, Weinheim

Moreover the usage of screening techniques based on independent physical methods prevents from discovering PAIN compounds (PAIN: Pan Assay Interference) and covalent binders.[21] The different compounds were tested for binding to Hdm2 by performing a series of NMR titrations with isotopically enriched ^{15}N-Hdm2.[22] Strong binding of a compound to its target is indicated by signal splitting in a heteronuclear single quantum coherence (HSQC) spectrum, whereas a signal shift indicates weaker binding. Figure 4 A–C shows NMR data of Hdm2 titrated with PB12 as an example of slow chemical exchange and Figure 3 of the Supporting Information shows similar spectra with PB2 diastereomers as an example of fast chemical exchange. Additionally we used our recently introduced antagonist-induced dissociation assay (AIDA), a fast one-dimensional NMR method to determine K_d values (Figure 4 C and Supporting Information, Figure 4),[23] which are in agreement with the fluorescence polarization data shown in Figure 4 D.

From the HSQC spectra we calculated the K_d^{NMR} values for *syn*-PB2 and *anti*-PB2 to be (3 ± 1) μM and ca. 40 μM, respectively. Table 1 shows a selection of other Hdm2 binding compounds with their K_d values, ranging from 60 μM down to less than 1 μM. Due to the inherent requirements of the Hdm2 binding pocket, the PB compounds are highly hydrophobic and most of the active PB compounds show a low total polar surface area (TPSA, Supporting Information, Table 2), most probably resulting in low water solubility, an unfavorable quality of compounds designed to become drugs. According to our binding model of PB2, the methyl ester group is not involved in binding, but rather remains exposed to the solvent (Figure 3). Therefore, we reasoned that derivatization of the ester bond by amidation could potentially improve water solubility and binding affinity. Indeed, conversion of PB2 derivative PB2a to amide PB11 (Scheme 2) improved the potency of the imidazoline scaffold as well as its water solubility, as judged by the NMR experiments and the TPSA (Table 1 and Supporting Information, Table 2 and Figure 6).

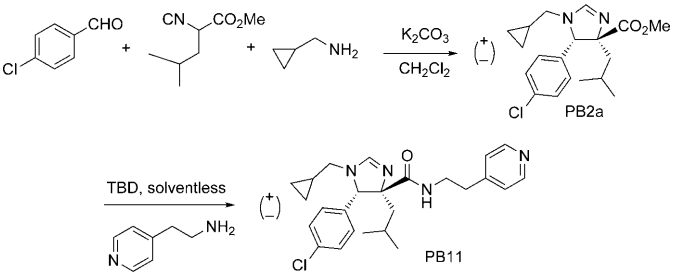

Scheme 2. One-pot synthesis of imidazoline PB2a by an Orru-3CR and optimization by amidation yielding derivative PB11 with improved affinity and water solubility (TBD = 1,5,7-triazabicyclo[4.4.0]dec-5-ene).

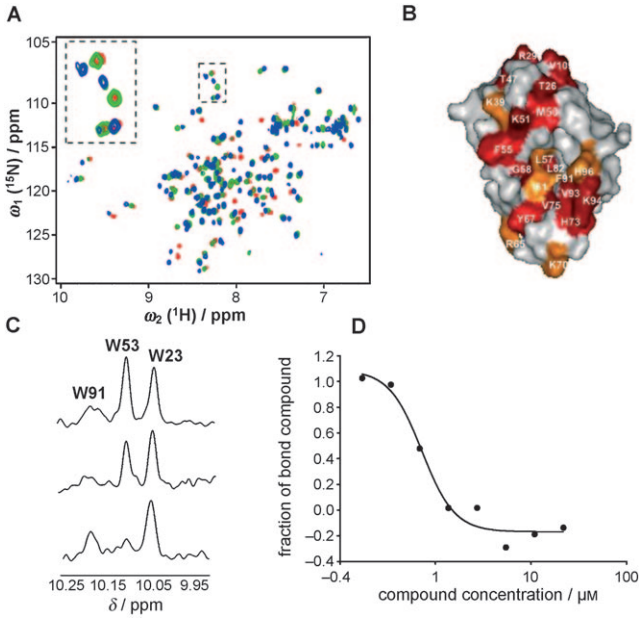

Figure 4. Screening of the activity of PB12. A) ^{1}H-^{15}N HSQC spectra of Hdm2 (1–125) titrated with increasing amounts of PB12. Red spectrum: apo-Hdm2; green spectrum: approximately 40% saturation of Hdm2 with PB12 (the spectrum shows slow chemical exchange that is typical for strong interactions with submicromolar K_d values); blue spectrum: Hdm2 fully saturated with PB12. B) Perturbation plot of PB12. C) AIDA experiment: the concentration of p53 released from the p53/Hdm2 complex by the antagonist is proportional to the height of the HN indole peak of W23(p53). Bottom: downfield-shifted NMR signals of the p53/Hdm2 complex (20 μM); middle: approximately 70% of dissociation of the complex upon addition of PB12 to the complex in a 1:1 molar ratio; top: signals of free p53. D) Study of PB12 by the fluorescence polarization assay.[11,26]

We have introduced a new process for predicting and producing antagonists of the cancer-relevant p53/Hdm2 protein–protein interaction. This approach differs substantially from currently used techniques, including high-throughput screening, fragment-based approaches, structure-based design or computational screening of compound libraries. Classical fragment-based drug discovery approaches, for example, are strong in detecting weakly, however efficiently binding small molecular units which serve as starting points to assemble more-potent druglike compounds, however with no straightforward synthetic pathway.[27] Herein, MCR chemistry was used to synthesize more-potent leads starting from a fragment (= anchor). Thus a seamless pathway for the optimization of affinity and other important drug properties is predefined. Nutlin-3, for example, is synthesized in a sequential synthesis of more than eight steps whereas PB11 is accessible in only two steps from commercially available starting materials.[28] The compounds collected in Scheme 1 are druglike and can be optimized regarding potency and physicochemical properties (Supporting Information, Figure 6). Certainly, this new approach, successful for one target example, demands further validation with different types of PPIs. Extensive optimization and in vitro and in vivo testing of optimized compounds of the different scaffolds reported herein are under way and will be reported in due course.

Received: March 5, 2010
Revised: May 4, 2010
Published online: June 23, 2010

 © 2010 Wiley-VCH Verlag GmbH & Co. KGaA, Weinheim

Keywords: antagonists · drug discovery · multicomponent reactions · p53/Hdm2 interaction · protein–protein interactions

[1] a) R. W. Spencer, *Biotech. Bioeng. Comb. Chem.* **1998**, *61*, 61 – 67; b) E. Jacoby, A. Boettcher, L. M. Mayr, N. Brown, J. L. Jenkins, J. Kallen, C. Engeloch, U. Schopfer, P. Furet, K. Masuya, J. Lisztwan in *Chemogenomics* (Ed.: E. Jacoby), Springer, Heidelberg, **2009**, pp. 173 – 194 (Series: *Methods in Molecular Biology*, Vol. 575).

[2] J. A. Wells, C. L. McClendon, *Nature* **2007**, *450*, 1001 – 1009.

[3] I. M. A. Nooren, J. M. Thornton, *EMBO J.* **2003**, *22*, 3466 – 3492.

[4] a) C. Tse et al., *Cancer Res.* **2008**, *68*, 3421 – 3428; b) K. Zobel, L. Wang, E. Varfolomeev, M. C. Franklin, L. O. Elliott, H. J. Wallweber, D. C. Okawa, J. A. Flygare, D. Vucic, W. J. Fairbrother, K. Deshayes, *ACS Chem. Biol.* **2006**, *1*, 525 – 533.

[5] a) A. A. Bogan, K. S. Thorn, *J. Mol. Biol.* **1998**, *280*, 1 – 9; b) I. S. Moreira, P. A. Fernandes, M. J. Ramos, *Proteins Struct. Funct. Genet.* **2007**, *68*, 803 – 812.

[6] a) A. Dömling, *Chem. Rev.* **2006**, *106*, 17 – 89; b) R. V. A. Orru, M. de Greef, *Synthesis* **2003**, 1471 – 1499; c) L. Weber, K. Illgen, M. Almstetter, *Synlett* **1999**, 366 – 374; d) C. Hulme, Y.-S. Lee, *Mol. Diversity* **2008**, *12*, 1 – 15; e) I. Ugi, A. Dömling, W. Hörl, *Endeavour* **1994**, *18*, 115 – 122; f) *Multicomponent Reactions* (Eds: J. Zhu, H. Bienaymé), Wiley-VCH, Weinheim, **2005**; g) B. Ganem, *Acc. Chem. Res.* **2009**, *42*, 463 – 472; h) J. D. Sunderhaus, S. F. Martin, *Chem. Eur. J.* **2009**, *15*, 1300 – 1308.

[7] P. H. Kussie, S. Gorina, V. Marechal, B. Elenbaas, J. Moreau, A. J. Levine, N. P. Pavletich, *Science* **1996**, *274*, 948 – 953.

[8] L. Meireles, A. Dömling, C. J. Camacho, *Nucl. Acids Res.* **2010**, DOI:10.1093/nar/gkq502.

[9] G. Pirok, N. Mate, J. Varga, J. Szegezdi, M. Vargyas, S. Dorant, F. Csizmadia, *J. Chem. Inf. Model.* **2006**, *46*, 563 – 568.

[10] a) P. R. Gerber, K. Müller, *J. Comput.-Aided Mol. Des.* **1995**, *9*, 251 – 268; b) P. R. Gerber, *J. Comput.-Aided Mol. Des.* **1998**, *12*, 37 – 51.

[11] G. M. Popowicz, A. Czarna, S. Wolf, K. Wang, W. Wang, A. Dömling, T. A. Holak, *Cell Cycle* **2010**, *9*, 1104 – 1111.

[12] I. Ugi in *Isonitrile Chemistry* (Ed.: I. Ugi), Academic Press, New York, **1971**, pp. 149 – 155.

[13] C. Kalinski, M. Umkehrer, S. Gonnard, N. Jäger, G. Ross, W. Hiller, *Tetrahedron Lett.* **2006**, *47*, 2041 – 2044.

[14] D. van Leusen, *Org. React.* **2001**, *57*, 417 – 666.

[15] a) R. S. Bon, C. Hong, M. J. Bouma, R. F. Schmitz, F. J. J. de Kanter, M. Lutz, A. L. Spek, R. V. A. Orru, *Org. Lett.* **2003**, *5*, 3759 – 3762; b) R. S. Bon, N. E. Sprenkels, M. M. Koningstein, R. F. Schmitz, F. J. J. Kanter, A. Dömling, M. B. Groen, R. V. A. Orru, *Org. Biomol. Chem.* **2008**, *6*, 130 – 137.

[16] M. Passerini, T. Bonciani, *Gazz. Chim. Ital.* **1933**, *63*, 138 – 144.

[17] M. Betti, *Gazz. Chim. Ital.* **1900**, *30*, 306 – 316.

[18] H. Staudinger, *Justus Liebigs Ann. Chem.* **1907**, *356*, 51 – 123.

[19] a) K. Gewald, E. Schinke, H. Böttcher, *Chem. Ber.* **1966**, *99*, 94 – 100; b) Y. Huang, A. Dömling, *Mol. Divers.* **2010**, DOI: 10.1007s11030-010-9229-6.

[20] R. Bossio, S. Marcaccini, R. Pepino, *Tetrahedron Lett.* **1995**, *36*, 2325 – 2326.

[21] a) J. B. Baell, G. A. Holloway, *J. Med. Chem.* **2010**, *53*, 2719 – 2740; b) D. Reed, Y. Shen, A. Shelat, A. Arnold, A. Ferreira, F. Zhu, N. Mills, D. Smithson, C. Regi, D. Bashford, S. Cicero, B. Schulman, A. G. Jochemsen, K. Guy, M. A. Dyer, *J. Biol. Chem.* **2010**, DOI: 10.1074/jbc.M109.056747.

[22] a) S. B. Shuker, P. J. Hajduk, R. P. Meadows, S. W. Fesik, *Science* **1996**, *274*, 1531 – 1534; b) M. Pellecchia, I. Bertini, D. Cowburn, C. Dalvit, E. Giralt, W. Jahnke, T. L. James, S. W. Homans, H. Kessler, C. Luchinat, B. Meyer, H. Oschkinat, J. Peng, H. Schwalbe, G. Siegal, *Nat. Rev. Drug Discovery* **2008**, *7*, 738 – 745.

[23] a) M. Krajewski, U. Rothweiler, L. D'Silva, S. Majumdar, C. Klein, T. A. Holak, *J. Med. Chem.* **2007**, *50*, 4382 – 4387; b) M. Bista, K. Kowalska, W. Janczyk, A. Dömling, T. Holak, *J. Am. Chem. Soc.* **2009**, *131*, 7500 – 7501.

[24] a) L. T. Vassilev, B. T. Vu, B. Graves, D. Carvajal, F. Podlaski, Z. Filipovic, N. Kong, U. Kammlott, C. Lukacs, C. Klein, N. Fotouhi, E. A. Liu, *Science* **2004**, *306*, 844 – 848; b) B. L. Grassberger, et al., *J. Med. Chem.* **2005**, *48*, 909 – 912.

[25] K. Ding, Y. Lu, Z. Nikolovska-Coleska, G. Wang, S. Qiu, S. Shangary, W. Gao, D. Qin, J. Stuckey, K. Krajewski, P. P. Roller, S. Wang, *J. Med. Chem.* **2006**, *49*, 3432 – 3435.

[26] A. Czarna, G. Popowicz, A. Pecak, S. Wolf, G. Dubin, T. Holak, *Cell Cycle* **2009**, *8*, 1176 – 1184.

[27] C. W. Murray, D. C. Rees, *Nat. Chem.* **2009**, *1*, 187 – 192.

[28] a) D. C. Fry, S. D. Emerson, S. Palme, B. T. Vu, C.-M. Liu, F. Podlaski, *J. Biomol. NMR* **2004**, *30*, 163 – 173; b) Z. Wang, J. Malgorzata, T. Lambros, S. Ferguson, R. Goodnow, *J. Pharm. Biomed. Anal.* **2007**, *45*, 720 – 729.

 © 2010 Wiley-VCH Verlag GmbH & Co. KGaA, Weinheim